energies

MDPI

Article

Failure-Mode-Based Health Assessment of Major Power Equipment in MVDC Converter Stations

Jeong-Sik Oh, Taehun Kim, Jaedeok Park, Byonghyeon An, Seungyun Lee and Teasik Park *

Department of Electrical Engineering, Mokpo National University, Muan 58554, Republic of Korea; ferdinet105@naver.com (J.-S.O.); kaeu123@naver.com (T.K.); asfgd2000@naver.com (J.P.); shfmql12@mokpo.ac.kr (B.A.); seungyun8970@naver.com (S.L.)
* Correspondence: tspark@mnu.ac.kr

Abstract

Medium-voltage direct current (MVDC) converter stations integrate conventional power equipment and power-electronic components with distinct failure and degradation characteristics, making unified health assessment challenging. This study proposes a failure-mode-based health assessment method for major MVDC converter-station equipment. Major equipment is selected through risk priority number (RPN) analysis, while equipment health is independently evaluated using failure mode and effects analysis (FMEA), cross matrices, and condition indicators. The relationships between equipment failure modes and condition indicators are systematically established using FMEA and cross matrices. The selected indicators are classified into five condition grades using indicator-specific thresholds, and a folding function is applied to determine a representative health index (HI) by prioritizing the most severely degraded indicator. The proposed method is evaluated using 10 transformer cases derived from fault and condition assessment datasets and five submodule cases constructed from independent IGBT and capacitor accelerated degradation datasets. The transformer results generally exhibit assessment trends comparable to existing condition assessments, although differences are observed in certain cases. The submodule results demonstrate that degradation information from different components can be integrated into a representative HI under the constructed degradation scenarios. These findings demonstrate the applicability of the proposed framework to heterogeneous condition indicators and provide a basis for extending health assessment to other MVDC converter-station equipment.

Keywords: MVDC; asset management; FMEA; health index

Academic Editor: Ramon Leyva

Received: 19 October 2026
Revised: 12 November 2026
Accepted: 24 November 2026
Published: 27 November 2026

Copyright: © 2026 by the authors. Licensee MDPI, Basel, Switzerland. This article is an open access article distributed under the terms and conditions of the Creative Commons Attribution (CC BY) license.

1. Introduction

With the increasing penetration of renewable energy sources and energy storage systems, along with advances in power electronics technology, conventional alternating current (AC)-dominated power systems are evolving to accommodate direct current (DC)-based sources and loads. In particular, medium-voltage direct current (MVDC) systems have attracted considerable attention as a promising next-generation distribution technology, as they can overcome the power transfer capacity limitations of conventional AC distribution networks while facilitating the efficient integration of DC-connected resources, such as photovoltaic generation, energy storage systems, data centers, and electric vehicle charging infrastructure [1–3].

Power equipment is continuously exposed to thermal, electrical, mechanical, and environmental stresses during operation, resulting in various degradation phenomena, including insulation deterioration, contact wear, and changes in electrical characteristics. In particular, the degradation of power electronic equipment is influenced not simply by its service age but also by operational stresses, such as loading conditions, temperature, switching conditions, and repeated thermal cycling. For example, the electrical characteristics of power semiconductor devices may change due to degradation of their packaging materials and semiconductor structures. Similarly, the condition parameters of capacitors in modular multilevel converter (MMC) submodules, such as capacitance and equivalent series resistance (ESR), may change under repeated charging and discharging cycles and thermal stresses. Consequently, assessing the condition of MVDC equipment solely based on service age has inherent limitations, highlighting the need for condition assessment using diagnostic information associated with actual degradation mechanisms [4–7].

A health index (HI) is a quantitative indicator that represents the overall condition of equipment by converting heterogeneous diagnostic and condition information into a common assessment scale and integrating the resulting values into a single index. In the field of power equipment asset management, various HI models have been developed, particularly for power transformers. These models assess the overall condition of equipment by assigning importance-based weights to multiple online and offline diagnostic parameters or by employing data-driven approaches. Such methods support maintenance and replacement decisions by representing multiple condition indicators through a single quantitative measure [8–10]. Specifically, existing transformer HI studies encompass weighted-score aggregation and data-driven or probabilistic approaches, while fuzzy-logic models have also been used to combine multiple diagnostic parameters [9,11]. Beyond transformers, reviews of power-electronic converter reliability and capacitor condition monitoring have addressed component-level degradation mechanisms, reliability assessment, and diagnostic indicators [12,13]. Research on MMC submodule failures has additionally examined fault diagnosis and fault-tolerant control [14]. These contributions provide important foundations for monitoring individual equipment types; however, their respective objectives and assessment outputs differ from a common equipment-level health grading procedure covering heterogeneous MVDC converter-station assets.

However, directly applying conventional HI assessment methods to MVDC converter stations presents several limitations. MVDC converter stations comprise not only conventional power equipment, such as transformers, but also components with distinct structures and degradation mechanisms, including power semiconductor devices, DC-link capacitors, and cooling systems. Consequently, the types and units of the applicable diagnostic parameters vary considerably. Since each diagnostic parameter has its own normal operating range and degradation characteristics, equipment condition cannot be adequately represented through direct numerical comparisons or uniform normalization procedures. Furthermore, when a diagnostic parameter directly associated with a specific failure mode exhibits severe degradation, its influence may be reduced during aggregation with numerous other parameters indicating normal conditions. Therefore, an HI assessment framework for MVDC equipment should incorporate the relationships between failure modes and diagnostic information, transform heterogeneous diagnostic parameters into a common assessment scale, and prevent severe degradation in individual parameters from being masked during the aggregation process [2,8]. In particular, conventional weighted aggregation can attenuate the effect of a severely degraded indicator when many other indicators remain in acceptable condition; this is a limitation for applications in which the worst condition indicator is intended to govern a conservative maintenance-oriented assessment. Accordingly, the present work focuses on failure-

mode-informed indicator selection and transparent threshold-based classification, rather than claiming improved prediction accuracy over data-driven diagnostic methods.

To address these limitations, this study proposes a failure-mode-based health assessment framework for major power equipment in MVDC converter stations. First, the risks associated with equipment and failure modes are analyzed to identify critical assessment targets. Failure mode and effects analysis (FMEA) is then employed to systematically establish the relationships among major failure modes, their causes, and the corresponding diagnostic parameters. Subsequently, a threshold-based condition classification method is applied using physical and technical reference values to convert diagnostic information with different units and characteristics into a common five-level health assessment scale. Furthermore, a folding function-based representative health index is introduced to prioritize deteriorated conditions during the aggregation of multiple health indicators, thereby preventing severe degradation in individual parameters from being masked by other parameters indicating normal conditions. Finally, degradation scenarios involving major diagnostic parameters are investigated to evaluate the condition identification characteristics and applicability of the proposed framework. Unlike component-specific monitoring or fault-diagnosis approaches, the proposed procedure links failure modes to observable condition indicators through equipment-specific cross matrices and uses a common five-grade scale and a worst-condition-preserving Folding Function across the selected MVDC equipment categories.

Figure 1 shows the overall procedure of the proposed failure-mode-based health assessment framework for MVDC converter stations.

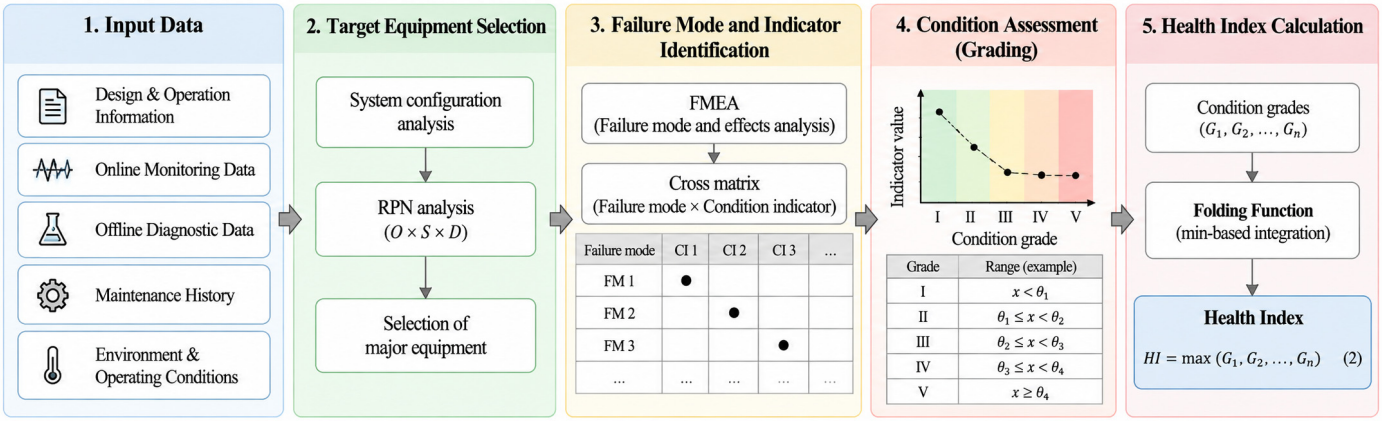


Figure 1. Framework of the Proposed Failure-Mode-Based Health Assessment Method for MVDC Converter Stations.

2. Characteristics of MVDC Converter Stations and Selection of Major Power Equipment

An MVDC converter station is a complex power system comprising both AC-side equipment connected to conventional AC distribution networks and DC-side equipment responsible for DC power conversion and distribution. In general, the AC yard includes equipment such as interface transformers, vacuum circuit breakers (VCBs), and reactors, while the DC yard comprises modular multilevel converter (MMC) valves, DC circuit breakers, and DC cables. In addition, various auxiliary components, including control systems, cooling systems, sensors, and connection accessories, are incorporated into the station. Unlike conventional AC substations, MVDC converter stations rely primarily on power electronic conversion equipment, with individual components exhibiting different

failure and degradation characteristics depending on their structures and operating principles [2,15].

Rather than applying the same level of health assessment to all equipment within an MVDC converter station, this study aims to prioritize critical equipment by considering the consequences of equipment failures on system operation, their likelihood of occurrence, and their detectability. To this end, Risk Priority Numbers (RPNs) are calculated based on failure occurrence, severity, and detectability, and major power equipment is selected according to the resulting RPN values. Subsequently, the structural characteristics and representative failure and degradation mechanisms of the selected equipment are analyzed to provide a technical basis for the failure-mode-based health assessment methodology proposed in the following section.

2.1. Configuration and Characteristics of MVDC Converter Stations

Medium-voltage direct current (MVDC) systems are generally classified as DC power systems operating at voltage levels ranging from 1.5 kV to below 100 kV. They are applied to distribution-level power networks within an intermediate voltage range between low-voltage direct current (LVDC) systems, which are primarily used for supplying residential and commercial consumers, and high-voltage direct current (HVDC) systems, which are designed for large-scale power transmission over long distances. MVDC systems can operate in conjunction with conventional AC distribution networks and efficiently integrate DC-based distributed energy resources and loads. Accordingly, MVDC technology has emerged as a promising solution for increasing the power transfer capacity and operational flexibility of existing distribution networks [1,2].

One of the fundamental differences between AC and DC distribution systems lies in their power conversion methods. In AC distribution systems, voltage levels can be relatively easily transformed using the principle of electromagnetic induction in transformers. In contrast, DC distribution systems require power electronic converters that regulate voltage magnitude and power flow direction through the switching operation of semiconductor devices. Therefore, unlike conventional AC substations, converter stations that perform AC/DC power conversion play a critical role in MVDC systems. These stations incorporate both AC-side and DC-side equipment to facilitate interconnection with existing AC distribution networks [16,17].

The configuration of an MVDC converter station may vary depending on its grid interconnection scheme and design objectives. However, it can generally be divided into an AC yard, which interfaces with the AC network, and a DC yard, which performs DC power conversion and distribution. The AC yard includes AC power equipment such as interface transformers, vacuum circuit breakers (VCBs), zig-zag transformers, and reactors, whereas the DC yard comprises DC power equipment such as MMC valves, DC circuit breakers, and DC cables. In addition, common auxiliary systems, including control systems, cooling systems, sensors, and connection accessories, are installed to support station operation and condition monitoring [18,19].

Although the point-to-point MMC-based MVDC configuration shown in Figure 2 is adopted as the reference system in this study, the proposed health assessment method is applied at the equipment level and is not inherently restricted to this topology. Its application to other MVDC configurations requires the identification of applicable equipment and the adjustment of equipment-specific failure modes, condition indicators, and assessment thresholds. For example, DC transmission cables may be absent in back-to-back converter configurations, whereas transformers and AC circuit breakers may not be applicable to fully DC networks without AC interfaces. Therefore, the scope of the assessment should be adapted to the equipment actually installed in each system.

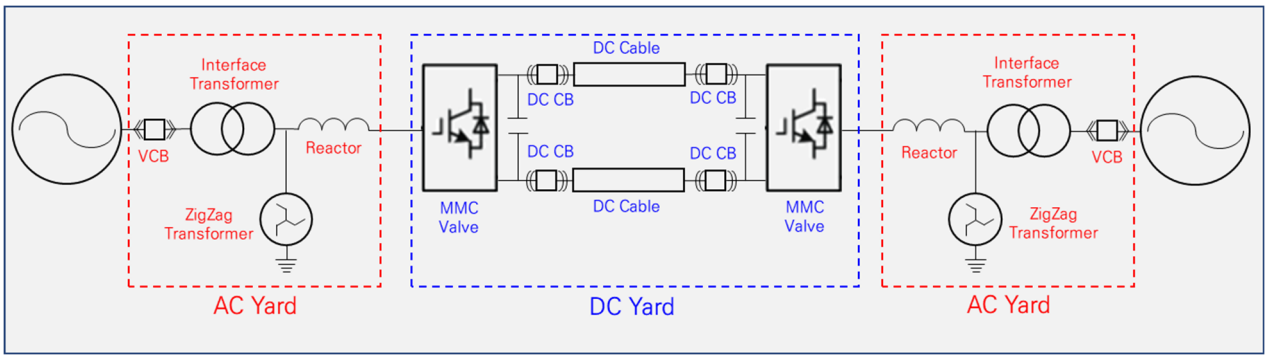


Figure 2. Single-Line Diagram of a Point-to-Point MVDC Converter Station Configuration.

Among these components, power converters serve as the core equipment of MVDC converter stations, converting AC power into DC power and vice versa. In particular, modular multilevel converters (MMCs), which are widely employed in modern voltage-source converter (VSC) systems, consist of multiple submodules connected in series to achieve the required DC voltage level. The operating conditions of the power semiconductor devices and capacitors within each submodule are directly related to the overall performance of the converter. Furthermore, unlike AC systems, DC systems do not exhibit periodic current zero crossings, making arc extinction during fault current interruption relatively challenging. Accordingly, hybrid DC circuit breakers combining mechanical and power electronic interruption mechanisms have been implemented in practical MVDC demonstration projects to address these DC fault interruption characteristics [18,19].

A demonstration project involving a ±35 kV MVDC converter station in South Korea employs a configuration that interconnects two AC distribution networks. The system is designed for bidirectional operation, allowing the converter stations to interchange their rectifier and inverter roles depending on operating conditions. In this configuration, the 22.9 kV AC voltage is stepped up through an interface transformer and subsequently converted into DC power using MMC valves, enabling power transmission at a DC voltage of ±35 kV. This configuration demonstrates that the operating conditions of not only conventional AC equipment but also power electronic devices, DC circuit breakers, and DC cables are directly associated with the stability of the overall MVDC system [3].

Therefore, MVDC converter stations integrate conventional AC power equipment with power-electronics-based DC equipment, each exhibiting distinct failure and degradation characteristics depending on its structure and operating principles. Compared with conventional AC substations, MVDC converter stations rely more heavily on power conversion and DC protection equipment. Furthermore, because individual components are subjected to different operating conditions and stresses, it is necessary to prioritize equipment for health assessment based on its criticality within the system rather than applying a uniform assessment approach to all components. Accordingly, the following section calculates the Risk Priority Numbers (RPNs) of major power equipment in MVDC converter stations to identify the critical equipment selected for health assessment in this study.

2.2. Selection of Major Power Equipment Based on RPN

MVDC converter stations consist of various components, including AC and DC power equipment, power converters, control systems, and auxiliary equipment. Since each component performs different functions within the system and exhibits distinct failure characteristics, it is necessary to prioritize equipment for health assessment based on its criticality rather than applying the same level of assessment to all components.

Therefore, this study employs the Risk Priority Number (RPN) method to identify major power equipment requiring prioritized health assessment within MVDC converter stations [20–23].

The RPN is an indicator used in Failure Mode and Effects Analysis (FMEA) to quantitatively determine the relative priority of failures based on three assessment factors: occurrence, severity, and detectability. Occurrence represents the likelihood of failure in a particular piece of equipment or component, while severity indicates the extent to which a failure affects equipment or system operation. Detectability represents the ability to identify abnormal conditions or potential signs of failure before an actual failure occurs, with higher scores assigned to equipment for which failure detection is more difficult [24].

The RPN is calculated as the product of occurrence, severity, and detectability, as expressed in Equation (1).

$$RPN = O \times S \times D \quad (1)$$

where O, S, and D represent failure occurrence, severity, and detectability, respectively. Each assessment factor was assigned a score using a ten-point rating scale based on the consensus-based evaluation procedure described below, with higher scores indicating a greater likelihood of failure occurrence, more severe consequences, or greater difficulty in detecting potential failures. Although the RPN provides a structured approach for prioritizing potential failures, its numerical value depends on the rating scales and assessment criteria adopted for occurrence, severity, and detectability. Moreover, different combinations of these three factors may yield identical RPN values despite representing different failure characteristics. Therefore, RPN values should be interpreted as relative priority indicators rather than direct estimates of failure probability. In this study, RPN results are considered together with equipment criticality and potential failure consequences when selecting major equipment for health assessment.

The occurrence (O), severity (S), and detectability (D) scores presented in Tables 1–3 were determined through a consensus-based assessment by the authors, considering equipment-specific failure characteristics reported in previous studies. Specifically, reported failure rates were used as reference information for assessing occurrence, with higher scores indicating a greater likelihood of failure. Severity was assessed by considering repair times and potential system-level consequences, with higher scores representing more significant operational impacts. Detectability was qualitatively evaluated based on the characteristics of the failure modes and the availability of applicable condition-monitoring and diagnostic techniques, with higher scores indicating greater difficulty in detecting potential failures. Based on these considerations, O, S, and D scores were assigned using a ten-point rating scale, and the corresponding RPN values were calculated using Equation (1).

It should be noted that the resulting RPN values represent a comparative risk assessment conducted in this study rather than values directly reported in the cited literature. Furthermore, the RPN analysis was employed solely to prioritize major equipment for subsequent health assessment and was not incorporated into the calculation of the proposed health index (HI). Therefore, potential uncertainties associated with the consensus-based RPN scoring do not directly propagate into the HI calculation for a given set of selected equipment.

Table 1. RPN Rank for VSC Station #1.

VSC Station 1						
Component	**Failure Rate**	**Repair Time**	**Occurrence**	**Severity**	**Detection**	**RPN**
DC Transmission Line	0.6613	7	10	8	8	640
Transformer	0.024	2160	8	9	5	360

Valves	0.5	4	10	6	6	360
AC Filters	0.54	6	10	7	4	280
Cooling Systems	0.27	12	10	7	3	210
Circuit Breaker	0.075	3	9	1	8	72
Ground Electrode	0.0042	10	5	1	6	30
DC Filters	0.001	5	4	1	7	28
Auxiliary Supply	0.0002	11	2	1	6	12
Station Controls	0.0002	1.5	2	1	3	6

Table 2. RPN Rank for VSC Station #2.

VSC Station 2						
Component	**Failure Rate**	**Repair Time**	**Occurrence**	**Severity**	**Detection**	**RPN**
DC Transmission Line	0.6613	988.8	10	9	8	720
Circuit Breaker	0.045	175.2	8	8	8	512
Transformer	0.1308	146	10	9	5	450
Valves	0.0813	36.5	9	7	6	378
AC Filters	0.1833	182.5	10	9	4	360
Station Controls	1.3096	1095	10	9	3	270
Cooling Systems	0.4352	175.2	10	9	3	270
DC Filters	-	-	-	-	-	-
Auxiliary Supply	-	-	-	-	-	-
Ground Electrode	-	-	-	-	-	-

Table 3. RPN Rank for VSC Station #3.

VSC Station 3						
Component	**Failure Rate**	**Repair Time**	**Occurrence**	**Severity**	**Detection**	**RPN**
DC Transmission Line	1.00	5	10	8	8	640
Valves	1.00	5	10	9	6	540
Transformer	0.07	1200	9	9	5	405
Circuit Breaker	0.015	50	7	7	8	392
AC Filters	0.05	300	9	6	4	216
DC Filters	0.05	300	9	3	7	189
Ground Electrode	0.01	10	7	2	6	84
Auxiliary Supply	-	-	-	-	-	-
Cooling Systems	-	-	-	-	-	-
Station Controls	-	-	-	-	-	-

Previous studies have examined the reliability and asset management of VSC-based DC systems from different perspectives. Joseph et al. [8] reviewed asset management strategies for power electronic converters in HVDC and FACTS applications, emphasizing condition monitoring, maintenance policies, and ageing and failure mechanisms. Ahmadi et al. [25] investigated the adequacy of hybrid AC/DC grids considering reliability-oriented MMC design, highlighting the importance of converter reliability in system-level performance. Contreras-Jiménez et al. [26] proposed a matrix-based reliability assessment method for multi-terminal HVDC systems, accounting for component failure probabilities and multiple operating states. Collectively, these studies support the consideration of equipment failure characteristics, operational consequences, and functional criticality when establishing health assessment priorities for MVDC converter stations. In this study, equipment failure rates and repair times reported in previous studies were reviewed as reference information, while the RPN assessment results were independently derived

through the consensus-based scoring procedure described above. A comparison of different VSC station cases, as presented in Tables 1–3, indicates that although the RPN rankings vary according to the assessed occurrence, severity, and detectability of equipment failures, equipment responsible for essential power conversion and transmission functions, such as DC transmission lines, converter valves, transformers, and circuit breakers, generally exhibits higher risk priorities. In contrast, auxiliary equipment, including filters, cooling systems, and station control systems, exhibits high RPN values in certain cases but shows considerable variation across cases. Furthermore, such equipment has different asset management characteristics compared with critical equipment constituting the main power transmission path [27,28].

Accordingly, this study does not employ RPN values as the sole criterion for equipment selection. Instead, the equipment selected for risk-based maintenance (RBM) is determined by comprehensively considering the RPN levels, functional criticality within the MVDC system, potential consequences of equipment failure on power supply, and the need for risk-based asset management. Consequently, five types of equipment, namely MMC valves, DC circuit breakers, DC cables, transformers, and vacuum circuit breakers (VCBs), were selected as RBM targets, as summarized in Table 4. These components constitute the main power paths of the AC and DC yards and are considered critical equipment because their failures are relatively likely to result in restrictions or interruptions of power conversion and supply functions. In contrast, wall bushings, DC disconnectors, zig-zag transformers, arm reactors, control and protection systems, and cooling systems were classified as equipment with relatively lower priorities for risk-based management or as equipment suitable for conventional condition-based maintenance (CBM) and time-based maintenance (TBM). Accordingly, these components were designated as CBM/TBM targets [29–31]. It should be noted that the RPN analysis is employed only to support the selection and prioritization of equipment for health assessment. The RPN values are not directly incorporated into the calculation of the final equipment health index. Instead, the proposed health assessment method determines equipment condition grades using failure-mode-related condition indicators, equipment-specific assessment thresholds, and the Folding Function described in Section 3. Consequently, uncertainties in RPN-based rankings may affect equipment selection priorities but do not directly propagate into the numerical calculation of the health grades for the selected equipment.

Table 4. RBM Target Selection Based on RPN Analysis.

Yard	Component	Maintenance Strategy
DC Yard	MMC Valve	RBM
	DC Circuit Breaker	RBM
	DC Cable	RBM
	Disconnecting Switch	CBM/TBM
AC Yard	Transformer	RBM
	VCB	RBM
	Zigzag Transformer	CBM/TBM
	Arm Reactor	CBM/TBM
Common Equipment	Control and Protection System	CBM/TBM
	Cooling System	CBM/TBM

3. FMEA-Based Health Index Assessment Method

This section proposes a failure-mode-based health assessment method for quantitatively evaluating the condition of major power equipment in MVDC converter stations. Since equipment health cannot be adequately assessed using measurements from a single

diagnostic parameter, it is necessary to comprehensively consider the relationships between potential equipment failure modes and the condition indicators that can reflect these failure modes [9,10].

To this end, Failure Mode and Effects Analysis (FMEA) was performed on transformers, vacuum circuit breakers (VCBs), MMC valves, DC circuit breakers, and DC cables, which were selected as risk-based maintenance (RBM) targets in the previous section. Through FMEA, the major failure modes, failure causes, and failure effects of each equipment type were identified, and condition indicators capable of representing equipment conditions were subsequently selected based on these results.

The RPN analysis described in Section 2.2 was used to support equipment selection, whereas the health assessment presented in this section evaluates the condition of the selected equipment independently of the RPN values.

The relationships between the identified failure modes and condition indicators were then analyzed and organized into a cross matrix. This approach systematically represents the relationships in which a single failure mode can be observed through multiple condition indicators and a single condition indicator can be associated with multiple failure modes.

For the selected condition indicators, thresholds were established based on equipment-specific testing standards, manufacturer recommendations, initial measurement values, and criteria reported in the relevant literature. To evaluate condition indicators with different units and characteristics on a common scale, each indicator was classified into five condition levels, ranging from 1 to 5, with higher levels indicating more advanced degradation.

Finally, a folding function was applied to aggregate the individual condition levels into a single representative value. When a simple averaging method is employed, severe degradation in certain condition indicators may be masked by other indicators representing normal conditions. Therefore, this study calculates a representative health index by prioritizing the condition level associated with the most severe degradation.

Accordingly, the representative health index is determined from the condition ratings of the selected diagnostic indicators rather than from the RPN-based equipment rankings.

Accordingly, the proposed failure-mode-based health assessment framework consists of four sequential steps: FMEA, mapping of failure modes to condition indicators, threshold-based condition classification, and calculation of a representative health index using the folding function.

3.1. Failure Mode and Effects Analysis of Major Equipment

In this study, Failure Mode and Effects Analysis (FMEA) was performed on transformers, vacuum circuit breakers (VCBs), submodules, DC circuit breakers, and DC cables, which were selected as risk-based maintenance (RBM) targets in the previous section [32,33].

Since MMC valves consist of multiple submodules containing power semiconductor devices and capacitors, the FMEA of MMC valves was conducted at the submodule level to identify the principal component-level failure modes.

FMEA is a systematic method for identifying potential failure modes of equipment and analyzing their causes and effects. In this study, failure modes, causes, and effects were analyzed based on the major components and functions of each equipment type. The principal failure characteristics were then summarized based on the relevant literature and previously reported failure cases [30,32,34].

For transformers, failure modes associated with insulation degradation, thermal abnormalities, and winding faults were analyzed, focusing on the insulation and winding

systems. For VCBs, the analysis focused on vacuum deterioration, reduced arc interruption performance, closing and opening malfunctions, and mechanical degradation. For submodules, insulated-gate bipolar transistors (IGBTs) and capacitors were identified as the major components, and electrical degradation, thermal stress, packaging and interconnection degradation, and changes in capacitance were selected as the principal failure modes [4,7,35,36].

For DC circuit breakers, the major failure modes included loss of interruption capability, failure and short-circuit faults of power semiconductor devices, insulation degradation, and deterioration of energy absorption components. For DC cables, conductor faults, insulation degradation, sheath and screen defects, and joint and termination defects were identified as the principal failure modes [37–40].

The detailed failure modes, causes, and effects identified through the FMEA of each equipment type are presented in Appendix A. In the subsequent analysis, condition indicators capable of monitoring the identified failure modes were selected based on the FMEA results, and the relationships between failure modes and condition indicators were systematically analyzed.

3.2. Mapping of Failure Modes and Condition Indicators

To utilize the failure modes identified through FMEA for practical condition assessment, it is necessary to select condition indicators capable of monitoring the occurrence or progression of degradation associated with each failure mode. However, a single failure mode may be monitored through multiple condition indicators, while a single condition indicator may be associated with multiple failure modes. Therefore, in this study, the relationships between failure modes and condition indicators were organized into a cross matrix to systematically represent these many-to-many relationships [9,33].

In the cross matrix, diagnostic and condition information capable of monitoring changes associated with each failure mode was mapped to the major failure modes of the corresponding equipment. The relationships between failure modes and condition indicators were classified as either direct or supplementary associations according to their degree of relevance. This approach enables the consideration of not only condition indicators that directly respond to specific failure modes but also those commonly associated with multiple failure modes. Accordingly, the cross matrix serves as a basis for selecting condition indicators associated with the identified failure modes, rather than assigning numerical weights or calculating equipment health indices at this stage.

Table 5 presents the relationships between the major failure modes of transformers and condition indicators, including winding resistance, insulation resistance and polarization characteristics, tan delta, partial discharge, sweep frequency response analysis (SFRA), insulating oil breakdown voltage, and dissolved gas analysis (DGA). Since transformers may experience different degradation mechanisms in various components, including insulation systems, windings and cores, connections, and on-load tap changers (OLTCs), it is necessary to comprehensively monitor failure modes using multiple diagnostic parameters rather than relying on a single condition indicator [10,41].

Table 5. Transformer Cross Matrix [32,33].

Failure Modes and Failure Types
Insulation Degradation
Partial Discharge and Electromagnetic Defects
Mechanical Deformation
Short Circuit and Arcing
Connection and Resistive Overheating
OLTC Malfunction

Condition Indicators						
Winding Resistance Test	▲	●	●	▲		
Insulation Resistance/Polarization Test			▲		▲	●
Insulation Deterioration Test/Tan Delta					▲	●
Partial Discharge Measurement			▲		●	▲
SFRA Test			▲	●		
Insulating Oil Breakdown Voltage Test			▲		▲	●
Dissolved Gas Analysis (DGA)	▲	●	●		▲	●
Excitation Current Test			▲	▲		▲
Dynamic Resistance Measurement (OLTC)	●		▲			

※ Note: ● indicates a strong relationship between a failure mode and a condition indicator, whereas ▲ indicates a moderate relationship.

Table 6 presents the mapping between condition indicators and failure modes associated with vacuum deterioration, reduced arc interruption performance, closing and opening malfunctions, and mechanical degradation in vacuum circuit breakers (VCBs). The selected indicators include diagnostic information related to main circuit dielectric withstand capability, main circuit resistance, vacuum integrity, and mechanical operation, enabling the assessment of both electrical performance and mechanical operating characteristics [35,42,43].

Table 6. VCB Cross Matrix [35,42].

Failure Modes and Failure Types				
Vacuum Defect and Degradation				
Reduced Arc-Extinguishing Capability				
Closing/Opening Function				
Mechanical Performance Degradation				
Condition Indicators				
Main Circuit Dielectric Withstand Test			▲	●
Main Circuit Resistance Measurement	▲		●	
Vacuum Integrity Test				●
Mechanical Operation Test	●	●	▲	

※ Note: ● indicates a strong relationship between a failure mode and a condition indicator, whereas ▲ indicates a moderate relationship.

As described in Section 3.1, the submodule-level analysis represents the failure characteristics of the principal internal components of MMC valves, which were selected as major equipment in Section 2.2. Table 7 presents the relationships between major degradation mechanisms and condition indicators associated with power semiconductor devices and capacitors in submodules. Electrical and thermal degradation of power semiconductor devices can be monitored using indicators such as $V_{CE(on)}$, $V_{GE(th)}$, and I_{GES}, while capacitor degradation can be assessed through changes in capacitance and equivalent series resistance (ESR). In particular, since a submodule consists of power semiconductor devices and capacitors with different degradation mechanisms, it is important to incorporate multiple condition indicators into a unified assessment framework [4–7].

Table 7. Sub-Module Cross Matrix [4,7].

Failure Modes and Failure Types		
Catastrophic Failure		
Performance Degradation		

Packaging/Interconnection Degradation				
Intermittent Fault				
Condition Indicators				
$V_{CE(on)}$	▲	▲	●	▲
$V_{G(th)}$	●		●	
I_{CES}	●	●		▲
Temperature	▲	●	▲	▲
ESR Measurement	▲		●	
Capacitance Measurement			●	

※ Note: ● indicates a strong relationship between a failure mode and a condition indicator, whereas ▲ indicates a moderate relationship.

Table 8 presents the mapping between condition indicators and major failure modes of DC circuit breakers, including loss of interruption capability, failure and short-circuit faults of power semiconductor devices, insulation degradation, and deterioration of energy absorption components. Since the interruption performance of DC circuit breakers is directly influenced by not only mechanical operating characteristics but also the electrical and thermal conditions of power semiconductor devices, the assessment framework incorporates semiconductor-related condition indicators in addition to insulation and operational tests [37,38].

Table 8. DC CB Cross Matrix [37,38].

Failure Modes and Failure Types					
Loss of Interruption Function					
Device Failure/Short Circuit					
Physical Performance Degradation					
Reduced Energy Absorption Capability					
Insulation Performance Degradation					
Condition Indicators					
Main Circuit Dielectric Withstand Test	●				
Vacuum Integrity Test	●				
Mechanical Operation Test			●		●
$V_{CE(on)}$		▲	●	●	▲
$V_{G(th)}$			●	▲	▲
Hot-Spot Measurement	▲	●	▲		
Leakage Current Measurement	▲	●			

※ Note: ● indicates a strong relationship between a failure mode and a condition indicator, whereas ▲ indicates a moderate relationship.

Finally, Table 9 presents the relationships between condition indicators and major failure modes of DC cables, including conductor faults, insulation degradation, sheath and screen defects, and joint and termination defects. Partial discharge, DC withstand voltage, tan delta, time-domain reflectometry (TDR), and sheath testing provide different perspectives on the insulation condition and structural abnormalities of DC cables. Accordingly, these condition indicators were combined to enable the assessment of major cable failure modes [39,40].

Table 9. DC Cable Cross Matrix [39,40].

Failure Modes and Failure Types					
Conductor Defect					
Cable Insulation Degradation					

Sheath/Screen Defect				
Joint/Termination Defect				
Condition Indicators				
Partial Discharge	●		▲	
DC Withstand Voltage Test	▲	▲	●	
Tan Delta	▲		●	
Time-Domain Reflectometry (TDR)	●	▲		●
Sheath Test	▲	●		

※ Note: ● indicates a strong relationship between a failure mode and a condition indicator, whereas ▲ indicates a moderate relationship.

Through the cross matrices presented in Tables 5–9, the relationships between the major failure modes of each equipment type and the corresponding condition indicators were systematically defined. Rather than simply listing available diagnostic parameters, this process provides a technical basis for selecting input variables for health assessment by explicitly identifying which failure modes are reflected by each condition indicator. The selected condition indicators are subsequently converted into five-level condition ratings, ranging from 1 to 5, using the threshold-based classification method described in Section 3.3. These ratings are then used as inputs for calculating the representative health index.

3.3. Threshold-Based Condition Classification

In this study, a threshold-based condition classification method was applied to quantitatively evaluate the measurement results of the condition indicators selected in Section 3.2. Since condition indicators vary in physical quantities, units, and measurement ranges depending on the equipment and diagnostic objectives, it is difficult to directly compare their measured values or incorporate them into a unified health assessment framework. Therefore, the measurement results of each condition indicator were converted into common condition ratings by comparing them with predefined thresholds [9,29].

The condition ratings were classified into five levels: Very Good, Good, Fair, Poor, and Very Poor, corresponding to integer values from 1 to 5, respectively. The assessment criteria were established such that higher ratings indicate more advanced degradation or abnormal conditions. The thresholds for each condition indicator were determined based on relevant testing standards, manufacturer recommendations, initial measurement values, design limits, and degradation criteria reported in previous studies. This approach enables heterogeneous condition information to be converted into a common assessment scale and subsequently used as standardized inputs for calculating the representative health index [10,29].

The threshold values are indicator-specific and should be interpreted according to the corresponding diagnostic characteristics and reference criteria, rather than as universally applicable limits for all equipment types.

Furthermore, per-unit (p.u.)-based relative assessment criteria were applied to certain condition indicators for which uniform absolute thresholds are difficult to establish. When equipment ratings, manufacturer specifications, or initial characteristics differ, the initial measurement values, manufacturer-recommended values, or design reference values were normalized to 1 p.u., and condition ratings were determined based on the relative changes in actual measurements. This approach reduces the influence of differences in absolute values among equipment types and manufacturers on condition assessment results, while enabling the progression of degradation to be compared using a common reference scale [41].

For indicators assessed using relative thresholds, the direction of degradation must also be considered, since deterioration may be represented by either an increase or a decrease from the reference value, depending on the physical characteristics of the indicator.

Table 10 presents the condition assessment criteria for transformers. The assessment framework incorporates dissolved gas analysis (DGA), insulating oil quality, electrical diagnostic tests, and on-load tap changer (OLTC) condition information. The concentrations of major gases identified through DGA reflect thermal and electrical abnormalities in insulation materials, while insulating oil breakdown voltage, dielectric loss, partial discharge, and insulation resistance are used to assess insulation degradation. In addition, winding resistance and excitation current are evaluated based on their deviations from initial measurement values, and changes in OLTC condition are classified into corresponding ratings to consider both the electrical and mechanical conditions of transformers [10,41].

Table 10. Transformer Health Evaluation Criteria [10,41].

Equipment	Subsystem	Indicator	Unit	Condition Criteria				
				Very Good (1)	Good (2)	Fair (3)	Poor (4)	Very Poor (5)
Transformer	DGA	H_2	PPM	≤100	100~700	700~1800	>1800	-
		C_2H_2		Not	0~1	1~9	9~35	>35
		C_2H_4		≤50	50~100	100~200	>200	-
		CH_4		≤120	120~400	400~1000	>1000	-
		C_2H_6		≤65	65~100	100~150	>150	-
		CO		≤350	350~570	570~1400	>1400	-
		CO_2		≤2500	2500~4000	4000~10,000	>10,000	-
	Oil Quality	Breakdown Voltage	kV	≥40	-	30~40	-	<30
	Diagnostic Tests	Dielectric Loss	%	≤0.1	0.1~0.2	0.2~0.3	0.3~0.5	>0.5
		Partial Discharge	pC	Not	-	0~5	5~10	>10
		SFRA	-	≤0.1	-	0.1~0.2	-	>0.2
		Insulation Resistance	MΩ	≥1000	-	-	-	<1000
		Winding Resistance	%	≤2	2~5	5~10	10~15	>15
		Excitation Current	%	≤10	10~25	25~50	50~100	>100
	OLTC	OLTC Operation	%	≤5	5~10	10~20	20~40	>40

Table 11 presents the condition assessment criteria for vacuum circuit breakers (VCBs). For VCBs, main circuit insulation resistance, contact wear, and contact resistance are used to evaluate the insulation and current-carrying conditions of the main circuit, while leakage current of the vacuum interrupter is used to assess vacuum deterioration. In addition, mechanical operation-related condition indicators, such as opening time, contact travel characteristics, and coil current, are incorporated to evaluate not only the electrical condition of the circuit breaker but also degradation of its operating mechanism [42,44].

Table 11. VCB Health Evaluation Criteria [42].

Equipment	Subsystem	Indicator	Unit	Condition Criteria				
				Very Good (1)	Good (2)	Fair (3)	Poor (4)	Very Poor (5)
VCB	Main Circuit	Insulation Resistance Test	MΩ	≥500	-	-	-	<500
		Contact Wear	mm	<2	-	2~3	-	>3

		Contact Resistance	p.u.	≤1.05	-	1.05~1.1	1.1~1.2	>1.20
	Vacuum Interrupter	Leakage Current	mA	<0.1	-	0.1~0.2	0.2~0.3	>0.3
	Mechanical Operation Test	Opening Time	p.u.	≤1.0	-	1.0~1.25	1.25~1.5	>1.5
		Contact Travel	p.u.	≤0.5	-	0.5~0.75	0.75~1.0	>1.0
		Coil Current Measurement	p.u.	≤1.05	1.05~1.15	1.15~1.3	1.3~1.5	>1.5

Table 12 presents the condition assessment criteria for submodules. Since insulated-gate bipolar transistors (IGBTs) and capacitors are the major components of a submodule, condition indicators were selected to reflect the degradation characteristics of each component. For IGBTs, $V_{CE(on)}$, $V_{GE(th)}$, and I_{GES}, were evaluated based on their deviations from reference values, while capacitor conditions were classified using changes in capacitance, equivalent series resistance (ESR), and temperature. By converting the measurement results of power semiconductor devices and capacitors, which exhibit different degradation mechanisms, into a common five-level condition rating scale, an integrated condition assessment at the submodule level was enabled [4–7,45].

Table 12. Sub-Module Health Evaluation Criteria [4,7].

Equipment	Subsystem	Indicator	Unit	Condition Criteria				
				Very Good (1)	Good (2)	Fair (3)	Poor (4)	Very Poor (5)
Sub-Module	IGBT	$V_{CE(on)}$	p.u.	≤1.05	-	1.05~1.15	-	>1.15
		$V_{G(th)}$	p.u.	≤1.2	-	1.1~1.2	-	>1.2
		I_{CES}	p.u.	<5	-	-	-	≥5
	Capacitor	Capacitance Loss	%	≤10	-	10~20	-	>20
		ESR Increase	%	≤50	-	50~180	-	>180
		Temperature	%	≤90	-	≤100	-	>100

Table 13 presents the condition assessment criteria for DC circuit breakers. Since the interruption performance of DC circuit breakers is influenced by the combined conditions of the main circuit insulation, power electronic circuits, and mechanical operating components, condition indicators were selected to reflect these characteristics. Main circuit insulation resistance and leakage current are used to evaluate insulation performance, while condition indicators associated with power electronic circuits are assessed based on their deviations from reference values to determine semiconductor degradation. In addition, operating time, the number of short-circuit operations, and coil current are incorporated to reflect the effects of repeated interruption operations and changes in mechanical operating characteristics [37,38].

Table 13. DC CB Health Evaluation Criteria [37].

Equipment	Subsystem	Indicator	Unit	Condition Criteria				
				Very Good (1)	Good (2)	Fair (3)	Poor (4)	Very Poor (5)
DC Circuit Breaker	Main Circuit	Insulation Resistance	MΩ	≥200	-	-	-	<200
		Leakage Current Test	mA	<0.1	-	0.1~0.2	0.2~0.3	>0.3
		Harmonic	p.u.	≤0.9	0.9~1.0	1.0~1.1	1.1~1.2	>1.2
	Electronic Circuit	$V_{CE(on)}$	p.u.	≤1.0	-	1.0~1.2	1.2~1.25	>1.25
		$V_{G(th)}$	p.u.	≤1.0	-	1.0~1.5	-	>1.5

		T_{on}, T_{off}	p.u.	≤1.0	-	1.0~1.2	1.2~1.25	>1.25
	Mechanical Operation Test	Operating Time	p.u.	≤1.0	-	1.0~1.25	1.25~1.5	>1.5
		Short-Circuit Operation Count	p.u.	≤0.5	-	0.5~0.75	0.75~1.0	>1.0
		Coil Current Measurement	p.u.	≤1.05	1.05~1.15	1.15~1.3	1.3~1.5	>1.5

Table 14 presents the condition assessment criteria for DC cables. For DC cables, partial discharge, insulation resistance, tan delta, time-domain reflectometry (TDR), and sheath test results were used to evaluate the conditions of conductors, insulation, sheaths, and screens. Partial discharge and tan delta reflect the degree of insulation degradation, while TDR is used to identify abnormalities in cables and joints based on deviations from reference signals. Furthermore, sheath testing is employed to assess the insulation condition of the external protective system, thereby enabling a comprehensive assessment of the major components of DC cables [39,40].

Table 14. DC Cable Health Evaluation Criteria [38].

Equipment	**Subsystem**	**Indicator**	**Unit**	**Condition Criteria**				
				Very Good (1)	**Good (2)**	**Fair (3)**	**Poor (4)**	**Very Poor (5)**
DC Cable	Conductor/Insulation	Partial Discharge (PD)	pC	Not detected	-	0~5	5~10	>10
		DC Insulation Resistance Test	-	Normal	-	-	-	Abnormal
		Tan Delta	-	≤0.001	0.001~0.004	0.004~0.008	0.008~0.01	>0.01
	Jacket	Insulation Resistance (TDR)	%	≤5	-	5~10	10~15	>15
	Screen/Sheath	Sheath Test	mA	≤1	1~5	5~10	10~20	>20

As described above, the threshold-based condition assessment criteria presented in Tables 10–14 enable condition indicators with different units and physical characteristics to be converted into a common five-level condition rating scale. This normalization process allows the degree of degradation to be compared on a consistent scale regardless of equipment type. Furthermore, it provides the basis for applying the individual condition ratings to the folding function described in Section 3.4 to calculate a representative health index for each equipment type.

3.4. Representative Health Index Using the Folding Function

In this study, a representative health index was calculated by aggregating the condition ratings of individual condition indicators to represent the overall condition of equipment. When multiple condition indicators are simply averaged to obtain a representative value, severe degradation in certain indicators may be masked by other indicators representing normal conditions [9].

To address this limitation, a folding function was applied. The folding function was designed to determine the representative health index by selecting the highest condition rating, corresponding to the most severe degradation, among the condition indicators associated with the equipment.

Let the condition ratings of individual condition indicators be denoted by $G_1, G_2, \cdots, G_n$. The representative health index is then calculated as follows:

$$HI_{rep} = \max(G_1, G_2, \cdots, G_n) \quad (2)$$

where HI_{rep} represents the representative health index of the equipment, and G_i denotes the condition rating determined for each condition indicator.

The condition ratings used as inputs to the folding function are obtained from the threshold-based classification procedure described in Section 3.3, with values ranging from 1 (Very Good) to 5 (Very Poor).

This approach ensures that severe degradation in a specific condition indicator is directly reflected in the overall health assessment of the equipment. Consequently, it prevents the masking of high-risk conditions that may occur in average-based assessment methods and enables a conservative health assessment based on the most severely degraded condition of the equipment.

Therefore, the representative health index should be interpreted as the most severe condition rating among the assessed indicators, rather than as an average measure of equipment degradation. The resulting representative health index expresses the current degradation condition of the equipment as a single quantitative value and provides a basis for evaluating the proposed method using the validation cases presented in Section 4.

4. Validation and Results of the Proposed Health Assessment Method

This section evaluates the applicability of the proposed failure-mode-based health assessment method and its assessment characteristics under different failure and degradation conditions. Since commercial applications and demonstration projects of MVDC converter stations remain limited, it is difficult to obtain sufficient datasets that integrate long-term operating histories of major equipment with condition information recorded before and after failures. Therefore, rather than using operational data from an entire converter station, this study evaluates the applicability of the proposed method using failure and degradation data obtained from previously published studies and publicly available datasets. Accordingly, the validation focuses on the applicability of the proposed assessment procedure to the available equipment-level datasets rather than demonstrating its performance across all five equipment types selected in Section 2.2.

The validation was conducted on two types of power equipment: transformers and submodules. For transformers, five dissolved gas analysis (DGA) failure cases provided by IEC TC 10 and five transformer condition assessment cases reported in previous studies were utilized. The IEC TC 10 dataset includes dissolved gas concentrations measured under different failure modes, while the literature-based dataset contains dissolved gas concentrations, insulating oil breakdown voltage (BDV), dielectric dissipation factor (DDF), and existing condition assessment results. These datasets were used to investigate the assessment characteristics of condition indicators associated with different failure modes and to evaluate the applicability of the proposed health assessment method using heterogeneous diagnostic parameters [9–11,46].

Next, accelerated degradation datasets for insulated-gate bipolar transistors (IGBTs) and capacitors were utilized to validate the proposed method for submodules, which are major components of MVDC converters. Based on IGBT degradation data from Hefei University and capacitor degradation data from NASA, five assessment cases were selected at approximately 10-cycle intervals over the range of 0–41 cycles [47,48]. Since the IGBT and capacitor measurements originate from separate accelerated degradation experiments, the combined cases are used to examine the response of the proposed assessment method to different component degradation levels rather than to represent the simultaneous ageing of components within an actual operating submodule. Changes in the electrical characteristics of IGBTs, decreases in capacitor capacitance, and increases in equivalent series resistance (ESR) were used as the primary condition indicators. These datasets were employed to investigate changes in health assessment results at different degradation levels [4–7]. For each validation case, the available diagnostic measurements were converted

into five-level condition ratings using the thresholds defined in Section 3.3, and the representative health index was subsequently determined using the folding function described in Section 3.4.

4.1. Validation Scenarios

To validate the applicability of the proposed failure-mode-based health assessment method, 10 transformer assessment cases and five submodule assessment cases were established. The validation utilized transformer failure and condition assessment data reported in previous studies, along with accelerated degradation test data for IGBTs and capacitors. The measurement parameters available in each dataset were mapped to the condition indicators defined in Section 3, and the assessment cases were categorized according to equipment-specific failure characteristics and dataset configurations. In particular, the transformer datasets were used to evaluate the applicability of the proposed method to different failure modes and condition assessment results, whereas the submodule dataset was designed to analyze changes in the representative health index according to the degradation levels of individual components.

For transformer validation, two datasets were utilized to establish a total of 10 assessment cases. The first dataset consisted of transformer DGA failure cases provided by IEC TC 10, from which five cases representing different internal failure modes were selected. DGA is a diagnostic method used to identify internal abnormalities by analyzing the types and concentrations of gases generated in insulating oil due to thermal and electrical faults within transformers. In this study, the concentrations of hydrogen (H_2), methane (CH_4), ethane (C_2H_6), ethylene (C_2H_4), and acetylene (C_2H_2) were used as condition indicators. The selected cases included failure modes such as tracking at grounding connections, localized overheating of bushings and insulating paper, damage to change-over selector contacts, and winding short circuits. Each failure mode exhibited a different distribution of dissolved gas concentrations. These cases were used to investigate how abnormal conditions in individual indicators associated with different failure modes are reflected in the representative health index. The corresponding data are presented in Table 15 [11,46].

Table 15. Transformer Validation Dataset (TC 10 Based) [46].

Transformer Case	Failure Mode	H_2	CH_4	C_2H_6	C_2H_4	C_2H_2
TR-1	Tracking to the grounding lug of central beam	60	10	4	4	4
TR-2	Hotspot on bushing	1	8	8	100	6
TR-3	Hotspot in paper	960	4000	1290	1560	6
TR-4	Burnt copper contacts in change-over selector	100	200	110	670	11
TR-5	Short-circuit in windings	1000	500	1	400	500

The second transformer dataset consisted of five condition assessment cases reported in previous studies. This dataset includes measurements of dissolved gas concentrations and electrical properties of insulating oil, together with equipment condition information assigned in the original assessments. In this study, ethane (C_2H_6), carbon monoxide (CO), carbon dioxide (CO_2), breakdown voltage (BDV), and dielectric dissipation factor (DDF) were selected as condition indicators. These indicators reflect degradation of internal insulation materials and the electrical characteristics of insulating oil. Therefore, unlike the first dataset, which relies solely on DGA gas concentrations, the second dataset enables health assessment using a combination of different diagnostic parameters. Furthermore,

the existing condition assessment results included in the original dataset were used to examine differences between the previously assigned conditions and the representative health indices calculated using the proposed method. The corresponding data are presented in Table 16 [11].

Table 16. Transformer Validation Dataset (Literature-Based) [11].

Transformer Case	Utility Estimation	C_2H_6	CO	CO_2	BDV	DDF
TR-6	Good	0	892	7038	48	0.249
TR-7	Worst	112	1843	2492	51.7	0.458
TR-8	Worst	26	1582	12,371	35	0.593
TR-9	Moderate	6	669	6764	49	0.1
TR-10	Bad	9	299	2348	46	0.221

For submodule validation, five assessment cases were established using IGBT degradation data from Hefei University and capacitor electrical overstress (EOS) accelerated degradation data from NASA. For IGBTs, collector–emitter voltage and gate threshold voltage were normalized to their initial reference values and used as condition indicators, while capacitance reduction and ESR increase rates were applied to capacitors. The assessment cases were constructed by combining IGBT measurements selected at degradation stages of 0, 10, 20, 30, and 41 cycles with corresponding capacitor degradation data. Because the IGBT and capacitor datasets were obtained from independent accelerated degradation experiments, the combined assessment cases represent constructed degradation scenarios rather than simultaneous ageing histories of components within an operating MMC submodule. These cases were used to analyze changes in the representative health index of submodules while considering the degradation characteristics of individual components. The validation data are presented in Table 17 [47,48].

Table 17. Sub-Module Validation Dataset (Hefei and NASA Based) [47,48].

Submodule Case	Degradation Stage	Vce	Vge	Cap	ESR
SM-1	Sample#1—0 Cycle	5.6512	1.8521	0.83	9.81
SM-2	Sample#2—10 Cycle	6.1618	1.8536	2.34	24.78
SM-3	Sample#1—20 Cycle	6.2389	1.8603	6.24	32.66
SM-4	Sample#3—30 Cycle	6.2974	1.8800	11.54	42.30
SM-5	Sample#1—41 Cycle	6.3124	1.9753	20.04	52.12

For the established assessment cases, individual condition ratings were determined by applying the indicator-specific thresholds defined in Section 3, and representative health indices were subsequently calculated using the folding function. For the transformer cases, health assessment results were analyzed under different failure modes and condition assessment datasets. For the submodule cases, changes in individual condition ratings and representative health indices were examined according to the degradation levels of IGBTs and capacitors. Therefore, the submodule cases were intended to examine how the proposed assessment procedure integrates different component degradation indicators, rather than to validate the physical ageing behavior of a complete MMC valve. Through these analyses, this study aimed to verify whether the proposed method can assess equipment failure and degradation conditions using heterogeneous condition indicators and appropriately reflect abnormal conditions in individual indicators in the representative health index.

4.2. Health Assessment Results

In this section, the proposed failure-mode-based health assessment method was applied to the validation datasets established in Section 4.1, and its assessment characteristics were analyzed by comparing the results with actual failure modes and existing condition assessment results. The measured values of each condition indicator were converted into five-level condition ratings, ranging from 1 to 5, using the thresholds defined in Section 3. The folding function was then applied to determine the representative health index (HI) of each equipment item based on the highest condition rating, corresponding to the most severe degradation. The assessment results for the IEC TC 10-based transformer failure cases are presented in Table 18.

Table 18. TC 10 Based Dataset Health Assessment Result.

Case	H_2	CH_4	C_2H_6	C_2H_4	C_2H_2	Health Index
TR-1	1	1	1	1	3	3
TR-2	1	1	1	2	1	2
TR-3	3	4	4	4	3	4
TR-4	1	2	3	4	4	4
TR-5	3	3	1	4	5	5

Compared with the actual failure modes, TR-1 and TR-2, which experienced tracking at grounding connections and localized overheating of bushings, respectively, exhibited relatively favorable condition ratings. In contrast, TR-3 to TR-5, which experienced localized overheating of insulating paper, damage to change-over selector contacts, and winding short circuits, respectively, were classified as being in poor condition, with HI values ranging from 4 to 5. In particular, TR-5, which experienced a winding short circuit, was assigned the highest HI value of 5, indicating that the severe internal fault was reflected in the resulting health assessment. These results demonstrate that the proposed method can incorporate abnormal conditions of individual indicators associated with different failure modes into the representative HI.

However, the relatively favorable ratings of TR-1 and TR-2, despite their documented failure modes, indicate that the representative HI depends on the diagnostic indicators available for each case and their corresponding assessment thresholds.

The assessment results for the literature-based transformer condition assessment cases are presented in Table 19. In the previous study, transformer conditions were classified into five levels: Excellent, Good, Moderate, Bad, and Worst, which are comparable to the five-level health assessment scale adopted in this study. The results show that TR-7 and TR-8, both classified as Worst in the original assessment, were assigned HI values of 4 and 5, respectively, indicating poor conditions. TR-9, originally classified as Moderate, was assigned an HI value of 3, consistent with the previous assessment. Meanwhile, TR-6 and TR-10, originally classified as Good and Bad, respectively, were both assigned an HI value of 3 using the proposed method. Although differences in condition ratings were observed in some cases, the proposed method generally exhibited assessment trends comparable to those of the existing condition assessment results. These findings indicate that the proposed method can produce health assessment results that are comparable to those obtained using an existing five-level condition assessment framework [9]. The differences observed for TR-6 and TR-10 suggest that the proposed method and the reference assessment do not necessarily assign identical condition ratings, even when applied to the same transformer cases. Therefore, the comparison should be interpreted as an examination of the consistency of assessment trends rather than a demonstration of exact agreement between the two methods.

Table 19. Literature-Based Dataset Health Assessment Result.

Case	C_2H_6	CO	CO_2	BDV	DDF	Health Index
TR-6	1	3	3	1	3	3
TR-7	4	4	1	1	4	4
TR-8	3	4	4	3	5	5
TR-9	1	3	3	1	1	3
TR-10	1	1	1	1	3	3

Figure 3 compares the transformer health assessment results obtained from the literature-based method and the proposed method. Although the five condition levels defined in the previous study do not exactly correspond to those adopted in the proposed method, both methods exhibit generally similar trends in assessing transformer health conditions. This suggests that the proposed method can provide health assessment results that are broadly consistent with existing assessments, despite differences in the classification criteria.

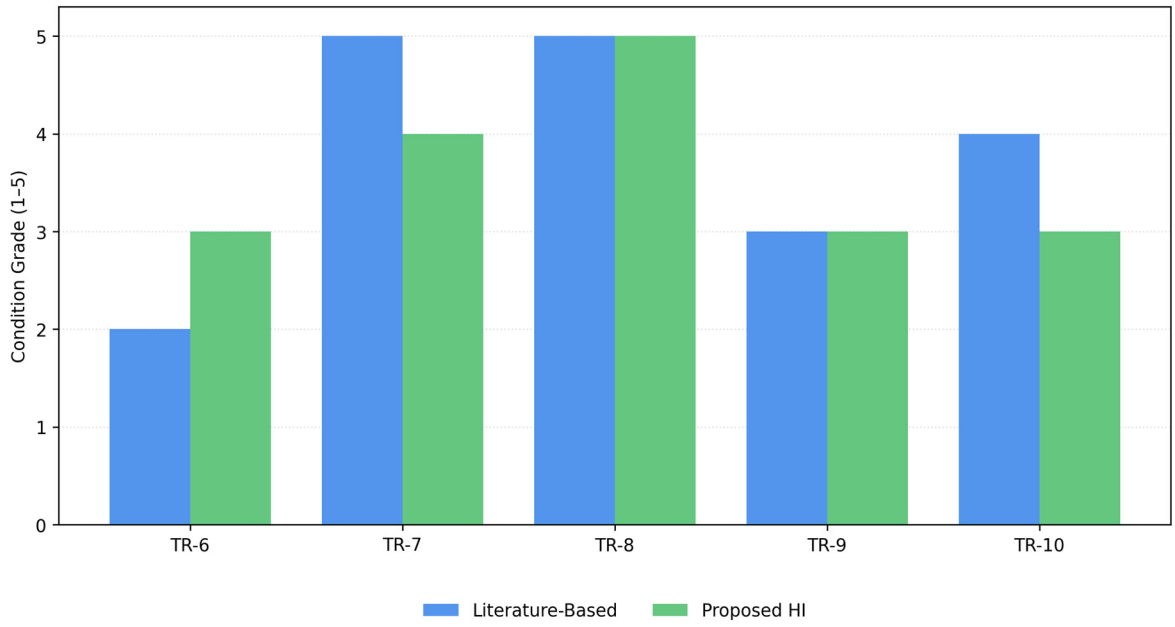


Figure 3. Comparison of Transformer Health Assessment Results Between the Literature-Based and Proposed Methods.

The assessment results for the accelerated degradation cases of submodules are presented in Table 20. In the initial condition, SM-1, all condition indicators exhibited favorable conditions, resulting in an HI value of 1. As degradation progressed, the representative HI increased to 3 and subsequently reached 5 at the final assessment stage, SM-5. In particular, changes in the electrical characteristics of the IGBT were reflected in the representative HI during the early degradation stages. As capacitor degradation progressed, accompanied by a decrease in capacitance and an increase in equivalent series resistance (ESR), the capacitor condition determined the representative HI at the final assessment stage. These results demonstrate that the proposed method can evaluate changes in submodule health by integrating condition information from components exhibiting different degradation characteristics. As the submodule cases were constructed from independent IGBT and capacitor degradation datasets, the observed HI progression reflects the

response of the proposed assessment method to the selected degradation scenarios and should not be interpreted as a measured ageing trajectory of an actual MMC submodule.

Table 20. Hefei- and NASA-Based Dataset Health Assessment Results.

Case	Vce	Vge	Cap	ESR	Health Index
SM-1	1	1	1	1	1
SM-2	3	1	1	1	3
SM-3	3	1	1	1	3
SM-4	3	1	3	1	3
SM-5	3	1	5	3	5

Overall, the proposed method reflected major abnormal conditions in the representative HI when evaluated against actual transformer failure modes and existing condition assessment results. Furthermore, the accelerated degradation cases of submodules exhibited a progressive deterioration in health condition with increasing degradation stages. In particular, the results demonstrate that the proposed method can assess the failure and degradation conditions of major equipment by converting heterogeneous condition information into a common condition rating scale and incorporating the most severely degraded condition indicator into the representative HI.

Nevertheless, because the folding function selects the highest condition rating, the representative HI reflects the most severely degraded assessed indicator rather than the average condition of all components. Its interpretation therefore depends on the coverage of relevant failure modes by the selected condition indicators.

5. Conclusions

This study proposed a failure-mode-based health assessment method for quantitatively evaluating the condition of major power equipment in MVDC converter stations. Considering the characteristics of MVDC systems, which integrate conventional power equipment and power-electronics-based equipment, major failure modes were identified through equipment-specific Failure Mode and Effects Analysis (FMEA). A health assessment framework was then established based on the relationships between the identified failure modes and corresponding condition indicators.

In the proposed method, the relationships between failure modes and condition indicators were systematically defined using cross matrices, and the condition of each indicator was classified into five levels based on predefined thresholds. Subsequently, the individual condition ratings were aggregated using a folding function to calculate a representative health index (HI) for each equipment item. This approach enables the integration of condition indicators with different characteristics into a unified assessment framework while ensuring that the effects of degradation in individual indicators associated with specific failure modes are reflected in the representative HI.

To validate the applicability of the proposed method, a total of 15 failure and degradation cases involving transformers and submodules were investigated. For transformers, DGA failure cases provided by IEC TC 10 and condition assessment cases reported in previous studies were utilized. Comparisons with actual failure modes and existing five-level condition assessment results demonstrated that the proposed method reflected major abnormal conditions and exhibited generally similar health assessment trends. However, differences between the proposed and reference assessments in certain transformer cases indicate that the results should be interpreted as evidence of methodological applicability rather than exact agreement with existing assessments. For submodules, accelerated degradation data for IGBTs and capacitors were employed. The representative HI

increased from 1 to 5 as degradation progressed, indicating that the degradation levels of individual components were reflected in the health assessment results. Since the submodule cases were constructed from independent component degradation datasets, these results demonstrate the response of the proposed assessment procedure to the selected degradation scenarios rather than the actual ageing behavior of an operating MMC submodule.

Overall, the proposed method provides a methodological basis for quantitatively assessing the health conditions of various types of equipment in MVDC converter stations by linking failure modes with condition information. However, the validation was limited to transformer and submodule cases, and further evaluation using operational data from other MVDC equipment types is required to establish the broader applicability of the proposed framework. As long-term operational and maintenance data from actual MVDC converter stations become available, the accuracy of the proposed method can be further improved by refining the thresholds of individual condition indicators and their relationships with failure modes. Furthermore, integrating the calculated HI with the probability and consequences of failure could extend the proposed framework to support maintenance prioritization and risk-based asset management decisions for MVDC power equipment.

Author Contributions: Conceptualization, J.-S.O. and T.P.; methodology, J.-S.O., B.A. and T.P.; validation, J.-S.O.; formal analysis, J.-S.O. and J.P.; investigation, J.-S.O. and T.K.; data curation, J.-S.O. and S.L.; writing—original draft preparation, J.-S.O.; writing—review and editing, J.-S.O. and T.P.; visualization, J.-S.O.; supervision, T.P.; project administration, T.P.; funding acquisition, T.P. All authors have read and agreed to the published version of the manuscript.

Funding: This work was supported by the Korea Institute of Energy Technology Evaluation and Planning(KETEP) and the Ministry of Climate, Energy & Environment(MCEE) of the Republic of Korea(No. 20225500000120). Basic Science Research Program through the National Research Foundation of Korea (NRF), funded by the Ministry of Education (RS-2025-25398164)

Data Availability Statement: The data used in this study were obtained from previously published studies and publicly available datasets. The transformer dissolved gas analysis (DGA) cases and literature-based transformer condition assessment cases were obtained from the sources cited in [46] and [11], respectively. The IGBT accelerated degradation data were obtained from the study cited in [47]. The capacitor electrical overstress (EOS) accelerated degradation dataset is publicly available through the NASA Open Data Portal (https://data.nasa.gov/dataset/accelerated-aging-in-electrolytic-capacitors-for-prognostics (accessed on 18 October 2026); dataset identifier: DASHLINK_792). The assessment cases and corresponding health assessment results derived from these sources are presented in Tables 15–20.

Acknowledgments: During the preparation of this manuscript, the authors used ChatGPT (OpenAI, GPT-6) for the purposes of English language editing, grammatical corrections, and improving clarity and readability. The authors have reviewed and edited the output and take full responsibility for the content of this publication.

Conflicts of Interest: The authors declare no conflicts of interest. The funders had no role in the design of the study; in the collection, analyses, or interpretation of data; in the writing of the manuscript; or in the decision to publish the results.

Abbreviations

The following abbreviations are used in this manuscript:

BDV	Break-Down Voltage
DGA	Dissolved Gas Analysis

ESR	Equivalent Series Resistance
FMEA	Failure Mode and Effects Analysis
HI	Health Index
IGBT	Insulated-Gate Bipolar Transistor
MMC	Modular Multilevel Converter
MVDC	Medium-Voltage Direct Current
RPN	Risk Priority Number
SM	Sub-Module
VCB	Vacuum Circuit Breaker
VSC	Voltage Source Converter

Appendix A

Appendix A presents the Failure Mode and Effects Analysis (FMEA) results for the major MVDC power equipment selected for health assessment in this study. The analysis covers transformers, vacuum circuit breakers (VCBs), submodules, DC circuit breakers, and DC cables. For each equipment type, the major failure modes, causes, and effects were systematically identified and summarized based on the functions and characteristics of its principal components. These results served as the basis for establishing the relationships between failure modes and condition indicators and selecting equipment-specific condition indicators for the health assessment framework presented in Section 3.

Table A1. Transformer FMEA.

Component	Failure Mode	Failure Effects	Failure Causes
Core	Core Grounding/Insulation Breakdown	Increased stray flux → Localized overheating, structural eddy-current losses, increased vibration and noise	Insulation degradation, contamination, oil ingress, mechanical assembly defects
Core	Multiple Core Grounding	Circulating current and localized overheating → Overheating, vibration, possible protection operation	Damage or loosening of grounding conductors, improper assembly
Core	Core Support/Clamping Looseness	Increased vibration → Risk of structural damage	Fastener loosening, prolonged vibration, thermal cycling
Windings	Winding Deformation/Displacement	Increased electrical stress and accelerated insulation degradation → Risk of internal fault	External through-fault current, insufficient clamping force
Windings	Inter-Turn Short Circuit	Local arcing and overheating → Accelerated insulation degradation and potential fire	Insulation ageing, localized overheating, manufacturing defects
Windings	Solid Insulation Deterioration	Partial discharge and reduced dielectric strength → Risk of flashover	Overloading, reduced cooling performance, moisture ingress
Winding Connections/Leads	Loose/Overheated Connection	Local overheating → Insulation degradation and arcing, resulting in lead damage	Loose bolted connections, poor workmanship, thermal expansion and contraction
Winding Connections/Leads	Lead Damage/Loosening	Increased vibration → Risk of ground fault or short circuit	Overcurrent, sustained vibration, installation errors
Winding Connections/Leads	Lead Support Damage	Lead deformation and insulation damage → Risk of internal fault	Structural ageing, sustained vibration
Solid Insulation	Moisture Ingress/Reduced Dielectric Strength	Increased dielectric loss (tan δ) and partial-discharge activity → Reduced dielectric withstand capability	Oil leakage, sealing defects, hygroscopic moisture absorption

Solid Insulation	Mechanical Damage (Cracking/Delamination)	Localized partial discharge and arcing paths → Risk of dielectric breakdown	Shipping/handling impact, damage during assembly
Solid Insulation	Reduced Degree of Polymerization (DP)	Reduced mechanical strength → Decreased winding support capability and increased insulation failure potential	Elevated hot-spot temperature, prolonged high-temperature operation, thermal ageing
Insulating Oil	Contamination/Sludge Formation	Reduced dielectric strength → Degradation of insulation performance	Particulate contamination, oxidation by-products, ageing products
Insulating Oil	Reduced Dielectric Strength	Flashover and overheating	Inadequate oil maintenance
Insulating Oil	Moisture/Gas Contamination	Increased partial discharge (PD) and gas generation → Accelerated insulation ageing	Oil leakage, overheating, oxidation
Bushing	External Contamination/Tracking	Surface discharge → Protection operation and risk of flashover	Salt and dust contamination, inadequate maintenance
Bushing	Internal Insulation Degradation/Partial Discharge	Partial discharge and dielectric breakdown → Risk of catastrophic failure	Moisture-induced degradation, internal defects, overvoltage
Bushing	Sealing Failure/Oil Leakage	Loss of insulating oil → Reduced dielectric performance and gasket contamination	Gasket ageing, sealing defects
OLTC	Contact Arcing/Carbonization	Increased contact resistance → Localized overheating and gas generation	Contact wear, excessive switching operations, high load current
OLTC	Repeated Switching/Persistent Arcing	Increased temperature → Insulation degradation, protection operation, and forced outage	Reduced contact area, carbon deposits
OLTC	OLTC Oil Degradation	Increased partial discharge and discharge activity → Electrical instability	Repetitive arcing, inadequate oil maintenance
OLTC	Tap-Changer Operating Mechanism Failure (Selector/Diverter Switch)	Failure of voltage regulation and risk of abnormal tap position	Mechanical defects, improper adjustment, interlock failure
OLTC	Drive Shaft/Motor Failure	Failure of tap operation and possible protection operation	Loose linkage, overload, mechanical wear
Cooling System	Fan/Pump Failure	Reduced cooling capacity → Increased temperature and accelerated insulation ageing	Overloading, ageing, mechanical wear
Cooling System	Radiator/Piping Blockage or Damage	Reduced cooling performance and risk of oil leakage	Contamination, corrosion, inadequate maintenance
Tank/Enclosure	Corrosion/Perforation	Oil leakage → Reduced insulation and cooling performance	Corrosive environment, coating deterioration
Gasket/Sealing	Oil Leakage/Poor Sealing	Loss of insulating oil and moisture ingress → Insulation degradation	Gasket ageing, improper assembly

Table A2. VCB FMEA.

Component	Failure Mode	Failure Effect	Failure Cause
Vacuum Interrupter	Vacuum Leakage	Insufficient withstand voltage in the open state	Bellows damage, micro-cracks
Vacuum Interrupter	Contact Welding	Failure to interrupt	Increased contact bounce, repeated high-current interruptions
Vacuum Interrupter	Contact Wear	Increased possibility of restrike during interruption	Contact erosion caused by arc energy accumulation
Vacuum Interrupter	Vacuum Deterioration	Degraded withstand voltage performance in the open state	Increased internal material outgassing
Main Contact	Interruption Failure	Loss of protection function	Contact welding, increased contact resistance
Operating Mechanism	Closing/Opening Failure	Circuit breaker operation failure	Coil overheating, bearing wear, degraded spring elasticity
Operating Mechanism	Driving Force Reduction and Failure	Degraded protection performance due to delayed operation	Increased mechanical friction caused by lubricant degradation
Operating Mechanism	Increased Operating Time	Possible protection coordination failure	Increased mechanical friction, poor rod alignment
Mechanical Linkage	Maloperation	Unintended opening/closing operation	Loose fasteners, vibration
Control Unit	Drive Signal Failure	Circuit breaker maloperation	Power loss, EMI effects, signal interruption due to defects or contamination
Control Unit	Maloperation	Unnecessary interruption	Control circuit noise, contact failure caused by corrosion and tracking
Entire Circuit Breaker	Reduced Reliability	Reduced system reliability	Accumulated degradation of mechanical components
Entire Circuit Breaker	Reduced Service Life	Increased maintenance cost	Mechanical wear caused by repeated switching operations

Table A3. Sub-Module FMEA.

Component	Failure Mode	Failure Effects	Failure Causes
IGBT	Loss of Gate Control	Increased switching losses and heat generation → Submodule current imbalance	Accumulated thermal and electrical overstress, thermal runaway
IGBT	Open-Circuit Failure	Failure to generate the required voltage level → Voltage imbalance	Bond-wire failure, interconnection failure
IGBT	Short-Circuit Failure	Overcurrent → Submodule damage and protection trip	Overcurrent events, insulation failure, thermal runaway
IGBT	Die-Attach Degradation	Increased junction temperature → Reduced lifetime	Power cycling, solder fatigue
IGBT	Degradation of Switching Characteristics	Increased switching losses → Reduced conversion efficiency	Gate-oxide degradation, changes in parasitic parameters
IGBT	Threshold-Voltage Drift	Reduced gate-drive margin → Increased switching losses and potential malfunction	Accumulated thermal stress, gate-oxide degradation, changes in parasitic parameters
IGBT	Intermittent Malfunction	Abnormal voltage levels → Potential protection trip	Gate-signal disturbance, parameter variation, poor electrical contact

Capacitor	Capacitance Degradation	Increased voltage ripple → Degraded voltage-balancing performance	Elevated temperature, corona discharge, electrode expansion
Capacitor	Open-Circuit Failure	Loss of submodule functionality → Bypass operation required	Poor electrode connection, thermal and mechanical stresses
Capacitor	Short-Circuit Failure	Rapid heat generation → Increased fire risk	Overvoltage, film-insulation damage
Capacitor	Increased Dissipation Factor	Increased self-heating → Accelerated ageing	Elevated temperature, increased dielectric losses
Capacitor	Dielectric Breakdown	Arcing → Protection operation	Contamination, moisture ingress, repetitive overvoltage
Gate Driver	Protection Malfunction	Failure to interrupt fault current → Submodule damage	Sensing-circuit failure, unstable isolated power supply

Table A4. DC CB FMEA.

Component	Failure Mode	Failure Effects	Failure Causes
Load Commutation Switch (LCS)	Open-Circuit Failure	Failure of fault-current commutation → Interruption failure	Control/protection malfunction, semiconductor overheating
Load Commutation Switch (LCS)	Increased On-State Resistance	Localized overheating and device degradation → Bypass operation required	Semiconductor ageing, degraded cooling performance
Load Commutation Switch (LCS)	Unintended Turn-On	Unintended current conduction → Reduced system reliability	Protection logic malfunction
Main DC Breaker	Turn-Off Failure	Interruption failure → Sustained fault current	Overcurrent, gate-drive malfunction
Main DC Breaker	Short-Circuit Failure	Device destruction → Circuit-breaker damage	Overvoltage, excessive \(di/dt\) stress
Commutation Branch	Uneven Voltage Sharing	Device overvoltage → Cascading device failure	Parameter mismatch, ageing
Ultra-Fast Disconnector (UFD)	Opening Failure	Failure of interruption sequence → Interruption failure	Operating-mechanism defect, control malfunction
Ultra-Fast Disconnector (UFD)	Delayed Opening	Increased interruption time → Increased energy stress on MOSA	Mechanical wear, reduced actuator performance
Ultra-Fast Disconnector (UFD)	Reduced Dielectric Withstand Capability	Restrike and external arcing	Contact degradation, insulation ageing
MOSA	Thermal Runaway	Failure of energy absorption → Circuit-breaker damage	Accumulated excessive energy
MOSA	Degradation	Reduced protective capability → Increased risk of repeated interruption failure	Repetitive interruption stress
MOSA	External Insulation Breakdown	External arcing → Secondary damage	Contamination, ageing
Residual Current Switch (RCS)	Opening Failure	Sustained residual current → MOSA overheating	Mechanical defect, control malfunction
Residual Current Switch (RCS)	Restrike	Increased thermal stress on MOSA	Contact damage, excessive transient recovery voltage (TRV)
Direct Current-Limiting Reactor	Insufficient Inductance	Rapid fault-current rise → Increased risk of interruption failure	Inadequate design
Direct Current-Limiting Reactor	Insulation Degradation	Ground fault → Loss of circuit-breaker protection capability	Thermal and electrical stresses

Table A5. DC Cable FMEA.

Component	Failure Mode	Failure Causes	Failure Effects
Conductor	Overheating/Open-Circuit Failure	Overloading, repetitive overcurrent, accumulated thermal stress	Increased conductor resistance → Loss of power transmission capability
Cable Insulation	Mechanical Damage	External impact, mechanical compression, excessive bending	Localized electric-field enhancement → Partial discharge (PD)
Cable Insulation	Moisture Ingress	Damage to outer sheath, inadequate sealing at joints/terminations, long-term moisture diffusion	Reduced dielectric strength → Accelerated insulation degradation
Cable Insulation	Electrical Ageing	Local defects, overvoltage stress, accumulated space charge	Partial discharge growth → Dielectric breakdown
Cable Insulation	Thermal Ageing	Prolonged high-temperature operation, inadequate heat dissipation	Reduced insulation lifetime
Metallic Sheath/Screen	Sheath Defect	Moisture ingress, soil environment, improper grounding, mechanical damage, corrosion	Degraded sheath performance → Increased electrical stress on insulation
Outer Sheath/Armour	External Damage	Excavation activities, external mechanical impact	Moisture ingress → Damage to secondary insulation
Joint	Interfacial Insulation Degradation	Poor workmanship, void formation, DC electric-field concentration, loss of mechanical pressure	Localized discharge → Cable-section outage
Termination	Insulation Breakdown/Tracking	Contamination, moisture, electric-field concentration, poor workmanship	Flashover → Cable outage
Bonding/Grounding	Bonding Failure	Grounding design errors, ageing	Abnormal sheath voltage → Protection failure
Cable System	Surge/Overvoltage Stress	Lightning, switching surges, inadequate protection coordination	Insulation damage → Increased risk of dielectric breakdown

References

References

1. International Electrotechnical Commission (IEC). *Medium Voltage DC (MVDC) Grids for an All-Electric Society*; IEC White Paper MVDC:2025-09(en); IEC: Geneva, Switzerland, 2025. Available online: https://webstore.iec.ch/en/publication/109247 (accessed on 18 October 2026).
2. Yu, Liang. *Medium Voltage DC Distribution Systems*; CIGRE Technical Brochure No. 875; CIGRE: Paris, France, 2022. Available online: https://www.e-cigre.org/publications/detail/875-medium-voltage-dc-distribution-systems.html (accessed on 18 October 2026).
3. Coffey, S.; Timmers, V.; Li, R.; Wu, G.; Egea-Àlvarez, A. Review of MVDC Applications, Technologies, and Future Prospects. *Energies* **2021**, *14*, 8294. https://doi.org/10.3390/en14248294.
4. Dimech, E.; Dawson, J.F. Electrical Parameters Characterization of Aged IGBTs by Thermo-Electrical Overstress. In Proceedings of the IECON 2018—44th Annual Conference of the IEEE Industrial Electronics Society, Washington, DC, USA, 21–23 October 2018; pp. 5924–5929. https://doi.org/10.1109/IECON.2018.8591088.
5. Susinni, G.; Rizzo, S.A.; Iannuzzo, F. Two Decades of Condition Monitoring Methods for Power Devices. *Electronics* **2021**, *10*, 683. https://doi.org/10.3390/electronics10060683.
6. Dimech, E.; Dawson, J.F. IGBT's Ageing and Its Impacts on the EM Conducted Emissions. In Proceedings of the 2024 International Symposium on Electromagnetic Compatibility (EMC Europe), Bruges, Belgium, 2–5 September 2024; pp. 1082–1087. https://doi.org/10.1109/EMCEurope59828.2024.10722359.
7. Kang, F.-S.; Song, S.-G. Failure Analysis of Capacitor for Sub-Module in HVDC. *J. Inst. Korean Electr. Electron. Eng.* **2018**, *22*, 941–947. https://doi.org/10.7471/ikeee.2018.22.4.941 (In Korean)

8. Joseph, T.; Ugalde-Loo, C.E.; Liang, J.; Coventry, P. Asset Management Strategies for Power Electronic Converters in Transmission Networks: Application to HVDC and FACTS Devices. *IEEE Access* **2018**, *6*, 21084–21102. https://doi.org/10.1109/ACCESS.2018.2826360.
9. Li, S.; Li, X.; Cui, Y.; Li, H. Review of Transformer Health Index from the Perspective of Survivability and Condition Assessment. *Electronics* **2023**, *12*, 2407. https://doi.org/10.3390/electronics12112407.
10. Cole, P.; MacArthur, T.L. *Condition Assessment of Power Transformers*; CIGRE Technical Brochure No. 761; CIGRE: Paris, France, 2019. Available online: https://www.e-cigre.org/publications/detail/761-condition-assessment-of-power-transformers.html (accessed on 18 October 2026).
11. Mharakurwa, E.T.; Goboza, R. Multiparameter-Based Fuzzy Logic Health Index Assessment for Oil-Immersed Power Transformers. *Adv. Fuzzy Syst.* **2019**, *2019*, 2647157. https://doi.org/10.1155/2019/2647157.
12. Wang, H.; Blaabjerg, F. Power Electronics Reliability: State of the Art and Outlook. *IEEE J. Emerg. Sel. Top. Power Electron.* **2021**, *9*, 6476–6493. https://doi.org/10.1109/JESTPE.2020.3037161.
13. Dang, D.-L.; Kwak, S. Review of Health Monitoring Techniques for Capacitors Used in Power Electronics Converters. *Sensors* **2020**, *20*, 3740. https://doi.org/10.*3390/s20133740.*
14. Xiao, Q.; Jin, Y.; Jia, H.; Tang, Y.; Cupertino, A.F.; Mu, Y.; Teodorescu, R.; Blaabjerg, F.; Pou, J. Review of Fault Diagnosis and Fault-Tolerant Control Methods of the Modular Multilevel Converter Under Submodule Failure. *IEEE Trans. Power Electron.* **2023**, *38*, 12059–12077. https://doi.org/10.1109/TPEL.2023.3283286.
15. *IEC 62747:2014*; Terminology for Voltage-Sourced Converters (VSC) for High-Voltage Direct Current (HVDC) Systems. International Electrotechnical Commission: Geneva, Switzerland, 2014. Available online: https://webstore.iec.ch/en/publication/7413 (accessed on 18 October 2026).
16. Fan, Y.; Chi, Y.; Li, Y.; Wang, Z.; Liu, H.; Liu, W.; Li, X. Key Technologies for Medium and Low Voltage DC Distribution System. *Glob. Energy Interconnect.* **2021**, *4*, 91–103. https://doi.org/10.1016/j.gloei.2021.03.009.
17. Qu, L.; Yu, Z.; Song, Q.; Yuan, Z.; Zhao, B.; Yao, D.; Chen, J.; Liu, Y.; Zeng, R. Planning and Analysis of the Demonstration Project of the MVDC Distribution Network in Zhuhai. *Front. Energy* **2019**, *13*, 120–130. https://doi.org/10.1007/s11708-018-0599-2.
18. Andersen, D.B.R.; Garnelo Rodriguez, M. Design of MMC Sub-Module for High-Power Testing Applications. Master's Thesis, Aalborg University, Aalborg, Denmark, 2021. Available online: https://projekter.aau.dk/design-of-mmc-sub-module-for-high-power-testing-applications-9e17a2a2.html (accessed on 18 October 2026).
19. de Sousa, G.J.M.; Heldwein, M.L. Concentrated Submodules Model for Modular Multilevel Converters. In Proceedings of the 2017 IEEE Southern Power Electronics Conference (SPEC), Puerto Varas, Chile, 4–7 December 2017; pp. 1–6. https://doi.org/10.1109/SPEC.2017.8333622.
20. *PAS 55-1:2008*; Asset Management—Part 1: Specification for the Optimized Management of Physical Assets. British Standards Institution: London, UK, 2008. https://doi.org/10.3403/30171836.
21. *ISO 55000:2024*; Asset Management—Vocabulary, Overview and Principles. International Organization for Standardization: Geneva, Switzerland, 2024. Available online: https://www.iso.org/standard/83053.html (accessed on 18 October 2026).
22. International Electrotechnical Commission (IEC). *Strategic Asset Management of Power Networks*; IEC White Paper Asset Management:2015-10(en); IEC: Geneva, Switzerland, 2015. Available online: https://webstore.iec.ch/en/publication/23388 (accessed on 18 October 2026).
23. *IEC TR 62978:2017*; HVDC Installations—Guidelines on Asset Management. International Electrotechnical Commission: Geneva, Switzerland, 2017. Available online: https://webstore.iec.ch/en/publication/27900 (accessed on 18 October 2026).
24. Rastayesh, S.; Bahrebar, S.; Blaabjerg, F.; Zhou, D.; Wang, H.; Sørensen, J.D. A System Engineering Approach Using FMEA and Bayesian Network for Risk Analysis—A Case Study. *Sustainability* **2020**, *12*, 77. https://doi.org/10.3390/su12010077.
25. Ahmadi, M.; Van der Sande, R.; Shekhar, A.; Bauer, P. Adequacy of Hybrid AC-DC Grids with Reliability Oriented Modular Multilevel Converter Design—A Case Study Using Modified RTS-24 Network. In *2024 IEEE 21st International Power Electronics and Motion Control Conference (PEMC)*; IEEE: Pilsen, Czech Republic, 2024. https://doi.org/10.1109/PEMC61721.2024.10726380.
26. Contreras-Jiménez, J.; Rivas-Dávalos, F.; Song, J.; Guardado, J. Multi-State System Reliability Analysis of HVDC Transmission Systems Using Matrix-Based System Reliability Method. *Int. J. Electr. Power Energy Syst.* **2018**, *100*, 265–278. https://doi.org/10.1016/j.ijepes.2018.02.008.
27. CIGRE Working Group B4.54. *Guidelines for Life Extension of Existing HVDC Systems*; CIGRE Technical Brochure No. 649; CIGRE: Paris, France, 2016. Available online: https://www.e-cigre.org/publications/detail/649-guidelines-for-life-extension-of-existing-hvdc-systems.html (accessed on 18 October 2026).

28. CIGRE Working Group B4.89. *Condition Health Monitoring and Predictive Maintenance of HVDC Converter Stations*; CIGRE Technical Brochure No. 982; CIGRE: Paris, France, 2026. Available online: https://www.e-cigre.org/publications/detail/982-condition-health-monitoring-and-predictive-maintenance-of-hvdc-converter-stations.html (accessed on 18 October 2026).
29. Distribution Network Operators (DNOs). *DNO Common Network Asset Indices Methodology*: Health & Criticality, Version 2.1; Distribution Network Operators: UK, 2021. Available online: https://www.ofgem.gov.uk/decision/decision-distribution-network-operators-common-network-asset-indices-methodology-0 (accessed on 18 October 2026).
30. Electricity Transmission Owners (NGET, SHE-T and SPT). *NOMs Methodology, Issue 18*; Electricity Transmission Owners: UK, 2018. Available online: https://www.ofgem.gov.uk/publications/decision-not-reject-modified-electricity-transmission-network-output-measures-noms-methodology-issue-18 (accessed on 18 October 2026).
31. AusNet Services. Asset Management Strategy: Electricity Distribution Network; Document No. AMS 20-01, Issue 23; AusNet Services: Southbank, VIC, Australia, 2025. Available online: https://www.aer.gov.au/documents/asd-ausnet-ams-20-01-asset-management-strategy-310125 (accessed on 18 October 2026).
32. Akbari, M.; Khazaee, P.; Sabetghadam, I.; Karimifard, P. Failure Modes and Effects Analysis (FMEA) for Power Transformers. In Proceedings of the 28th International Power System Conference, Tehran, Iran, 4–6 November 2013; pp. 1–7. Available online: https://www.researchgate.net/publication/324818642_Failure_modes_and_effects_analysis_FMEA_for_power_transformers (accessed on 18 October 2026).
33. Kaur, J.; Bhangu, N.S. Condition Monitoring of Power Transformer Using Failure Modes and Effects Analysis (FMEA). *Int. J. Innov. Res. Sci. Eng. Technol.* **2017**, *6*, 19108–19115. https://doi.org/10.15680/IJIRSET.2017.0609049.
34. Eyüboğlu, O.H.; Dindar, B.; Gül, Ö. Risk Assessment by Using Failure Modes and Effects Analysis (FMEA) Based on Power Transformer Aging for Maintenance and Replacement Decision. In Proceedings of the 2020 IEEE 2nd Global Power, Energy and Communication Conference (GPECOM), Virtual, Izmir, Turkey, 20–23 October 2020; pp. 251–255. https://doi.org/10.1109/GPECOM49333.2020.9247887.
35. Antoun, C. High Voltage Circuit Breaker and Power Transformer Failure Modes and Their Detection. In Proceedings of the 2018 Condition Monitoring and Diagnosis (CMD), Perth, WA, Australia, 23–26 September 2018; pp. 1–6. https://doi.org/10.1109/CMD.2018.8535655.
36. Wang, Y.; Zhang, L.; Chen, H.; Liu, X.; Li, J.; Gao, P. Failure Analysis of Vacuum Circuit Breaker with Permanent Magnet Actuator. In Proceedings of the 2022 3rd International Conference on Advanced Electrical and Energy Systems (AEES), Lanzhou, China, 23–25 September 2022; pp. 191–195. https://doi.org/10.1109/AEES56284.2022.10079600.
37. PROMOTioN Consortium. Fault Stress Analysis of HVDC Circuit Breakers; Deliverable D5.3, Version 2.0; PROMOTioN—Progress on Meshed HVDC Offshore Transmission Networks. 2016. Available online: https://www.promotion-offshore.net/fileadmin/PDFs/D5.3_Fault_Stress_Analysis_of_HVDC_Circuit_Breakers. (accessed on 18 October 2026).
38. PROMOTioN Consortium. Document on Failure Mode Analysis of HVDC Circuit Breakers; Deliverable D10.5; PROMOTioN—Progress on Meshed HVDC Offshore Transmission Networks. 2020. Available online: https://www.promotion-offshore.net/fileadmin/PDFs/D10.5_Document_on_failure_mode_analysis_of_HVDC_circuit_breakers.pdf (accessed on 18 October 2026).
39. Morshuis, P.H.F.; Cavallini, A.; Fabiani, D.; Montanari, G.C.; Azcarraga, C. Stress Conditions in HVDC Equipment and Routes to in Service Failure. *IEEE Trans. Dielectr. Electr. Insul.* **2015**, *22*, 81–91. https://doi.org/10.1109/TDEI.2014.004815.
40. Barghandan, A.; Saffari, S.; Sarfi, V. Failure Mode and Effects Analysis for MV XLPE Cable Systems. In Proceedings of the 29th International Power System Conference (PSC 2014), Tehran, Iran, 27–29 October 2014. Available online: https://www.researchgate.net/publication/321192693_Failure_mode_and_effects_analysis_for_MV_XLPE_cable_systems (accessed on 18 October 2026).
41. *IEC 60076-7:2018*; Power Transformers—Part 7: Loading Guide for Mineral-Oil-Immersed Power Transformers. International Electrotechnical Commission: Geneva, Switzerland, 2018. Available online: https://webstore.iec.ch/en/publication/34351 (accessed on 18 October 2026).
42. *IEEE Std C37.09-2018*; IEEE Standard Test Procedures for AC High-Voltage Circuit Breakers with Rated Maximum Voltage Above 1000 V. Institute of Electrical and Electronics Engineers: New York, NY, USA, 2018. Available online: https://standards.ieee.org/ieee/C37.09/5676/ (accessed on 18 October 2026).
43. Hsu, C.-C.; Frusque, G.; Muratovic, M.; Franck, C.M.; Fink, O. Vacuum Circuit Breaker Closing Time Key Moments Detection via Vibration Monitoring: A Run-to-Failure Study. In Proceedings of the 2022 IEEE International Conference on Systems, Man, and Cybernetics (SMC), Prague, Czech Republic, 9–12 October 2022; pp. 254–260. https://doi.org/10.1109/SMC53654.2022.9945354.

44. Kumpalavalee, S.; Suwanasri, T.; Suwanasri, C.; Phadungthin, R. D-Distance Technique to Determine Failure Probability of Power Circuit Breaker. *Energies* **2023**, *16*, 847. https://doi.org/10.3390/en16020847.
45. Qazi, J.; Ikeda, M. Failure Analysis of Capacitors and Inductors. In *Microelectronics Failure Analysis: Desk Reference*, 7th ed.; Gandhi, T., Ed.; ASM International: Materials Park, OH, USA, 2019; pp. 587–602. https://doi.org/10.31399/asm.tb.mfadr7.t91110587.
46. Kim, S.-W.; Kim, S.-J.; Seo, H.-D.; Jung, J.-R.; Yang, H.-J.; Duval, M. New Methods of DGA Diagnosis Using IEC TC 10 and Related Databases Part 1: Application of Gas-Ratio Combinations. *IEEE Trans. Dielectr. Electr. Insul.* **2013**, *20*, 685–690. https://doi.org/10.1109/TDEI.2013.6508773.
47. Liu, H.; Li, X.; Liu, Z. A Data-Driven Approach for IGBT Aging Degree Evaluation Based on Multi-Observation Sequence Particle Filtering and Support Vector Regression. *Mech. Adv. Mater. Struct.* **2025**, *32*, 765–776. https://doi.org/10.1080/15376494.2024.2355371.
48. Celaya, J.R.; Kulkarni, C.S.; Biswas, G.; Goebel, K. Towards a Model-Based Prognostics Methodology for Electrolytic Capacitors: A Case Study Based on Electrical Overstress Accelerated Aging. *Int. J. Progn. Health Manag.* **2012**, *3*, 1–19. https://doi.org/10.36001/ijphm.2012.v3i2.1364.

Disclaimer/Publisher's Note: The statements, opinions and data contained in all publications are solely those of the individual author(s) and contributor(s) and not of MDPI and/or the editor(s). MDPI and/or the editor(s) disclaim responsibility for any injury to people or property resulting from any ideas, methods, instructions or products referred to in the content.